Journal of Intelligent Material Systems and Structures

http://jim.sagepub.com/

Performance Characterization of In-plane Electro-thermally Driven Linear Microactuators

Yongjun Lai, Evgueni V. Bordatchev, Suwas K. Nikumb and Wensyang Hsu

Journal of Intelligent Material Systems and Structures 2006 17: 919

DOI: 10.1177/1045389X06061770

The online version of this article can be found at:
http://jim.sagepub.com/content/17/10/919

Published by:

http://www.sagepublications.com

Additional services and information for *Journal of Intelligent Material Systems and Structures* can be found at:

Email Alerts: http://jim.sagepub.com/cgi/alerts

Subscriptions: http://jim.sagepub.com/subscriptions

Reprints: http://www.sagepub.com/journalsReprints.nav

Permissions: http://www.sagepub.com/journalsPermissions.nav

Citations: http://jim.sagepub.com/content/17/10/919.refs.html

>> Version of Record - Oct 4, 2006

What is This?

Downloaded from jim.sagepub.com at NATIONAL CHIAO TUNG UNIV LIB on April 26, 2014

Performance Characterization of In-plane Electro-thermally Driven Linear Microactuators

YONGJUN LAI,[1,]** EVGUENI V. BORDATCHEV,[1,]* SUWAS K. NIKUMB[1] AND WENSYANG HSU[2]

[1]*Integrated Manufacturing Technologies Institute, National Research Council of Canada*
800 Collip Circle, London, Ontario N6G 4X8, Canada
[2]*Department of Mechanical Engineering, National Chiao-Tung University*
1001 Ta Hseuh Road, Hsin Chu, Taiwan, 30010, ROC

ABSTRACT: Static and dynamic electro-mechanical performance of a microactuator is a key factor in the functioning of an integrated microsystem composed of moving components such as optical shutters/switches, micropumps, microgrippers, and microvalves. Therefore, the development of such systems primarily focuses on the overall design and parameter optimization of an actuator as the major driving element with respect to the desired performance parameters, e.g., displacement, force, dimensional constraints, material, actuation principle, and method of fabrication. This study presents results on the static and dynamic electro-mechanical performance analysis of an in-plane electro-thermally driven linear microactuator. Each microactuator, having a width of 2220 μm and made of 25 μm thick nickel foil, consisted of a pair of cascaded structures. Connecting several actuation units in a series formed each cascaded structure. Several microactuators with a different number of actuation units were fabricated using the laser micromachining technology. The static performance of these microactuators was evaluated with respect to the maximum linear output displacements, actual resistance, applied current, and consumed electric power. The maximum displacements varied approximately from 3 to 44 μm, respectively, depending on the number of actuation units. The dynamic performance was studied as a response function on constant applied current with respect to the output displacements. In addition, the response time was evaluated for different applied currents and for actuators with 2, 4, and 6 actuation units. The microactuators' performance results are promising for applications in MEMS/MOEMS, microfluidic, and microrobotic devices.

Key Words: microactuator, in-plane motions, electro-thermal actuation, laser fabrication, static and dynamic electro-mechanical performance.

INTRODUCTION

THE action-oriented applications of microfluidic, micro-electro-mechanical, and micro-opto-electro-mechanical systems (MEMS and MOEMS) such as optical shutters, switches, micropumps, microgrippers, and microvalves require desired electro-mechanical performance parameters such as linear/rotary displacements and/or applied forces. These parameters are provided by the static and dynamic performance of a microactuator, which is a key functional component in the design of such systems with moving mechanisms. A reliable static performance of the microactuator is critical when a high-precision movement and/or precise grasping/holding actions are desired in such microsystems.

Four actuation principles are commonly used for the classification of MEMS/MOEMS microactuators: electrostatic, piezoelectric, electro-thermal, and based on shape memory alloy effect (Hsu, 2002). Each microactuator with certain actuation principles has its own advantages and disadvantages, and specific areas of applications. The typical electrostatic microactuators produce relatively small forces (<10 μN) and displacements (<5 μm) for applied voltage >50 V (Harness and Syms, 2000). A larger range of motion and force are achievable with higher applied voltage (Ye et al., 1998). Recently developed electrostatic microactuators with a larger force and motion still required a driving voltage >100 V (Grade et al., 2003). Piezoelectric actuators also require a higher voltage for generating force and motion, e.g., a voltage of 1000 V is necessary to produce 120 μm deflection (Debeda et al., 1999). Among the types of actuators mentioned above, electro-thermally driven microactuators are capable of producing longer strokes (>100 μm) and also are capable of handling

*Author to whom correspondence should be addressed.
**Now with Queen's University, Kingston, Ontario, Canada.
E-mail: evgueni.bordatchev@nrc.gc.ca
Figures 3 and 6 appear in color online: http://jim.sagepub.com

1045-389X/06/10 0919–11 $10.00/0 DOI: 10.1177/1045389X06061770
© 2006 SAGE Publications

Downloaded from jim.sagepub.com at NATIONAL CHIAO TUNG UNIV LIB on April 26, 2014

larger forces (>1 mN) with relatively lower applied voltage (typically <5 V) and within smaller design dimensions. Also, they are reliable, easily operated, and controllable. Furthermore, electro-thermal actuators are more suitable for microfabrication, handling of miniature parts and objects, assembly operations, and in-house packaging.

The nickel and polysilicon bimorph electro-thermally driven actuators (ETDA) were developed by Guckel et al. (1992) and Comtois et al. (1995). Other studies related to the improvements on bimorph ETDAs were performed by Huang and Lee (1999), and Hickey et al. (2002). Lai et al. (2004) pointed out that a single typical polysilicon bimorph ETDA can produce a maximum force and displacement of 6 μN and 6 μm, respectively. Further, an array of five bimorph ETDAs can only provide a maximum force of 17 μN while decreasing their total maximum displacement to 3 μm. Klaassen et al. (1995) and Williams et al. (1999) have demonstrated an ETDA with a different design configuration referred to as a '*V*' actuator. Typical forces that can be generated by such '*V*' actuators are up to several hundred micro Newton (Cragun and Howell, 1999; Sinclair, 2000; Que et al., 2001a) for a displacement <5 μm. To obtain larger displacements, motion amplifiers were implemented and attached to the '*V*' actuators (Lai et al., 2004). However, the use of motion amplifiers leads to dramatic drop of the output force with respect to the insignificant motion increment. For example, a '*V*' actuator comprised of polysilicon beams with 2×2 μm in cross-section and 200 μm of length, generated a displacement of 3 μm and a force of several hundred micro Newtons. After implementation of a motion amplifier, the maximum output force dropped to 3 μN while the maximum displacement increased only to 20 μm (Lai et al., 2004). The simulation results of the cascaded '*V*' shaped EDTAs using polysilicon and nickel reported by Hsu et al. (2002) showed larger displacements, typically >100 and 250 μm with 10 and 0.5 V, respectively. Therefore, the trade-off between output displacement and the force depends primarily on the design, kinematics, and material properties of the microactuator.

Recent developments in the microfabrication technologies (Hsu, 2002) extend a range of process options for the fabrication of miniature functional components and assembly of microsystems from traditional technologies borrowed from the semiconductor industry, including bulk micromachining, wet and dry etching processes, and surface micromachining and LIGA processes, to the laser micromachining, focused ion-beam, and μ-EDM processes. All these processes have different merits and limitations. For example, the popular MEMS surface micromachining processes, MUMPs (multi-user-MEMS-process), is able to produce MEMS devices with two structural layers having a thickness of 2 and 1.5 μm, respectively (Koester et al.). It is well known that such thin structures at a microscale are sensitive to ambient humidity. The laser micromachining technology is more suitable for rapid prototyping and in some cases for mass production of miniature functional components, microdevices, and microsystems with complex 2D/3D geometry having accuracy and precision within ±1 μm from a variety of materials (Braun and Zimmer, 2001; Bordatchev et al., 2002, 2004).

In this article, a set of in-plane, electro-thermally driven microactuators with 2, 4, 6, and 8 identical actuation units linked together forming two parallel cascaded structures, was fabricated from a nickel foil having a thickness of 25 μm using the laser micromachining technology. The static and dynamic electro-mechanical performance of these microactuators has been characterized systematically with respect to the maximum linear displacement and applied electrical parameters, such as power, current, and voltage.

MICROACTUATOR DESIGN

Figure 1 shows the detailed design of the microactuator, a single actuation unit, and fabricated microactuator prototype with two cascaded structures and eight actuation units in each structure. The geometrical dimensions of all the design elements are listed in Table 1. The actuator design is based on a multi-cascaded approach (Bordatchev et al., 2002; Hsu et al., 2002; Bordatchev and Nikumb, 2004) and consists of a pair of identical, in-plane, cascaded structures linked together at the top by a horizontal beam as motion platform. Each cascaded structure is formed by a serial connection of several basic actuation units which magnify the output in-plane displacements. A driving electric potential was applied between the two fixed electric pads (anchor 1 and 2) at the bottom of each cascaded structure. The actuation principle is based on the electro-thermal effect. When the electric current runs through the conductive structure of the microactuator it produces Joule heating, generating thermal expansion of all the individual elements and eventually the entire structure. As a result of the thermal expansion of all actuation units in cascaded structures, the motion platform moves forward producing output in-plane displacements and force. The symmetric monolithic structure was chosen to provide a symmetrical distribution of the voltage, temperature, and displacements along each vertical cascaded structure and the entire actuator. More detailed description of the design of similar microactuators can be found in Bordatcher et al. (2002) and Hsu et al. (2002). Also, description of the microactuators with similar designs can be found in (Gianchandani and Najafi, 1996; Que et al., 2001b; Lai et al., 2004; Luo et al., 2004, 2005; Syms et al., 2004).

Downloaded from jim.sagepub.com at NATIONAL CHIAO TUNG UNIV LIB on April 26, 2014

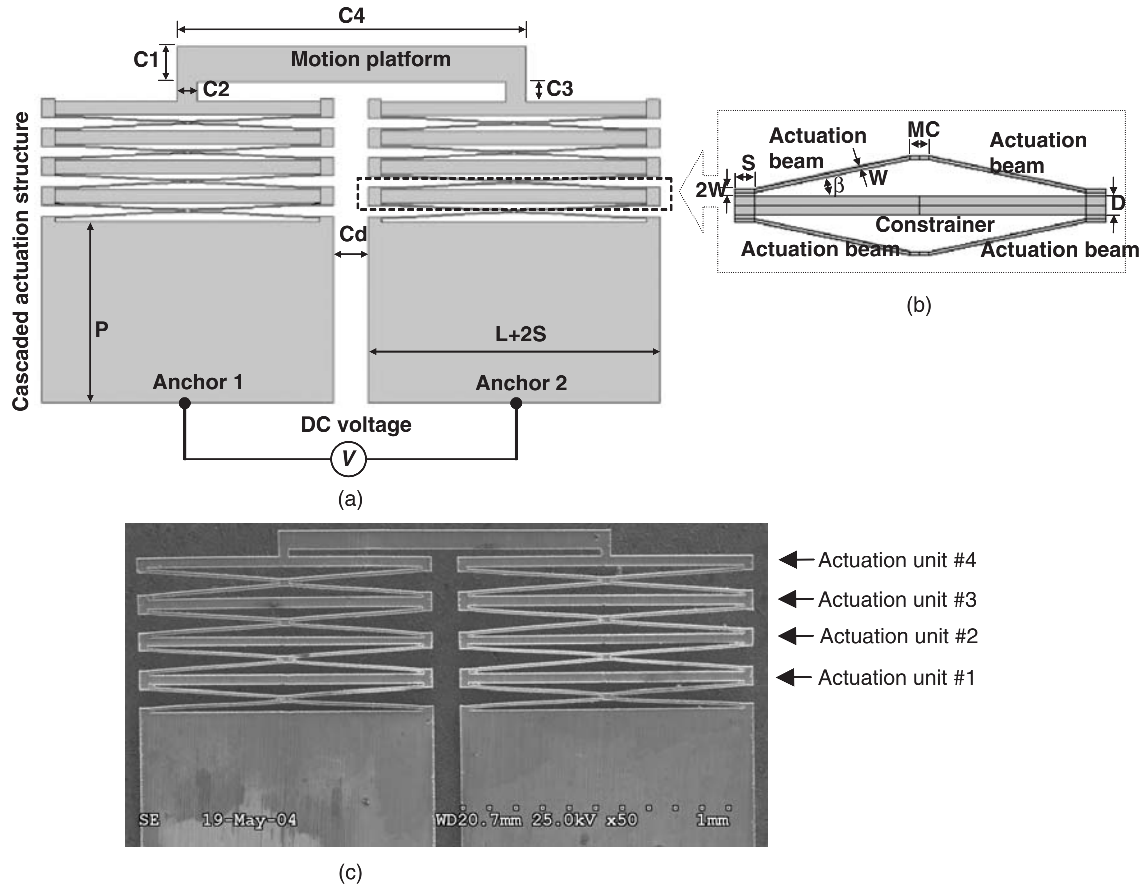

Figure 1. Detailed design and fabricated prototype of a microactuator with four actuation units: (a) design of an entire microactuator; (b) design of an actuation unit; and (c) fabricated microactuator prototype with 4 actuation units.

Table 1. Dimensions of the design elements (see Figure 1).

L	1000	C1	60
W	10	C2	30
β	5°	C3	30
D	30	C4	L + 2*S + C2 + Cd
S	30	P	500
MC	30	Cd	100

1. All dimensions in μm, except β, which is in degrees.
2. Anchor 1 and anchor 2 are electrical contact pads.

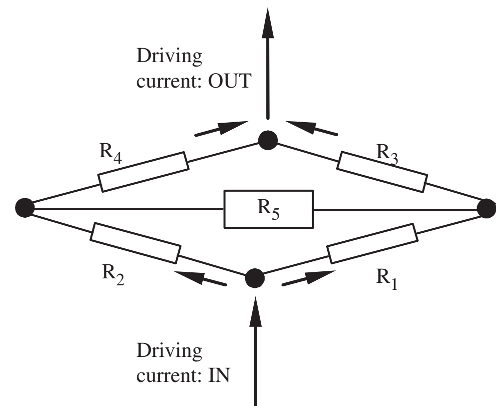

Figure 2. Electrical Wheatstone bridge of an actuation unit.

It is important to note that the design of the microactuator allows optimization of the structural aspects with respect to the desired displacements by selecting a certain number of actuation units and with respect to the desired force by choosing a set of number of the cascaded actuation structures.

Each actuation unit consists of two pairs of mirrored 'V' beams, called actuation beams, joined together at the inner ends as shown in Figure 1(b). The outer ends of the actuation beams are attached to a wider bar called constrainer referring to its functional purpose, described below. A design combination of two 'V' actuation beams and a constrainer is similar to a cascaded open toggle mechanism (Lai et al., 2004) with a difference that outer actuation beams are fixed to a substrate. Since the dimensions of the thin, long actuation beams are $10 \times 25\,\mu m$ (width to thickness) in cross-section, they have a higher electrical resistance compared to the wider constrainer with a cross-section of $30 \times 25\,\mu m$. Figure 2 shows an electric equivalent to the actuation unit as a Wheatstone bridge formed by the resistances of four actuation beams, R_1–R_4, and the constrainer, R_5. The four actuation beams have

Downloaded from jim.sagepub.com at NATIONAL CHIAO TUNG UNIV LIB on April 26, 2014

equivalent resistances (R_1–R_4) by design, and consequently, the bridge is always balanced. In the balanced Wheatstone bridge, no electrical current flows through the diagonal resistance, R_5, represented by the constrainer. In the fabricated prototypes, it was observed that the Wheatstone bridge was working under a well-balanced status with negligible current leakage through the constrainer. Therefore, under the Joule heating conditions, only the actuation beams, R_1–R_4, were expanded pushing forward the rest of the actuation units with respect to the fixed anchors. The Joule heat generated in the constrainer, R_5, was insignificant. The only source of thermal expansion of the constrainer is the heat transferred from the actuation beams causing expansion of the constrainer which may reduce microactuator efficiency slightly. As a result, the actuation beam expands significantly more than the constrainer during the electro-thermal heating stage. In addition, when the actuation unit is electrically heated, the actuation beam tends to expand in all directions evenly and the constrainer limits the expansion of the actuation unit in the horizontal direction. Consequently, the constrainer directs the primary displacements towards the desired vertical direction. When electrical potential was applied between the two anchors, the output displacement was generated from the summation of the responses of all the basic actuation units in one cascaded structure. The directions of motion can be outward (stretching mode) or inward (shrinking mode), depending on whether the actuation beams were under expansion or contraction.

Simulated electro-thermal performance of the microactuator shown in Figure 3 supports the above rationale in the design of a single actuation unit and an entire microactuator. The temperature distribution (Figure 3(a)) has significant variations and gradients. The maximum temperature rise occurs in the actuation beams and especially at the point of interconnection (point A on Figure 3(a)). Note that the temperature variation and gradient between the actuation beam and the constrainer is a major source of the electro-thermal actuation, because the overall temperature of all design elements of the microactuator is increasing significantly during the actuation. Figure 3(b) shows the temperature difference between three principal points of the actuation unit design during the actuation. The point A, at the interconnection of the actuation beams, point B, at the outer end of the constrainer, and point C, at the center of the constrainer represent temperatures T_A, T_B, and T_C, respectively. During the actuation, the difference $T_B(t) - T_C(t)$ becomes very small, changing from a maximum of 22°C to a minimum of 4°C. This result confirms the initial statement that the expansion of the constrainer does not reduce microactuator efficiency significantly. In comparison, the difference $T_A(t) - T_C(t)$, responsible for the microactuator performance, significantly increases from 0°C up to 137°C during 0.5 under an applied voltage of 0.6 V.

A set of microactuators with a different number of actuation units, in particular, 2, 4, 6, and 8, were fabricated from a 25 μm thick nickel foil using the laser microfabrication technology. The parameters of the laser-material removal process, such as laser power, pulse repetition rate, working distance, and feed rate, were optimized in order to achieve accuracy and precision of the fabricated prototype within ±1 μm. More detailed information on the laser micromachining system and fabrication challenges can be found in (Bordatchev and Nikumb, 2004; Bordatchev et al., 2002, 2004).

All ETDAs utilize the principle of thermal expansion resulting from Joule heating caused by the electric current flowing through the solid body of the actuator made of electro-conductive material. However in practice, a direct length increment available from the thermal expansion of a heated actuation beam is too

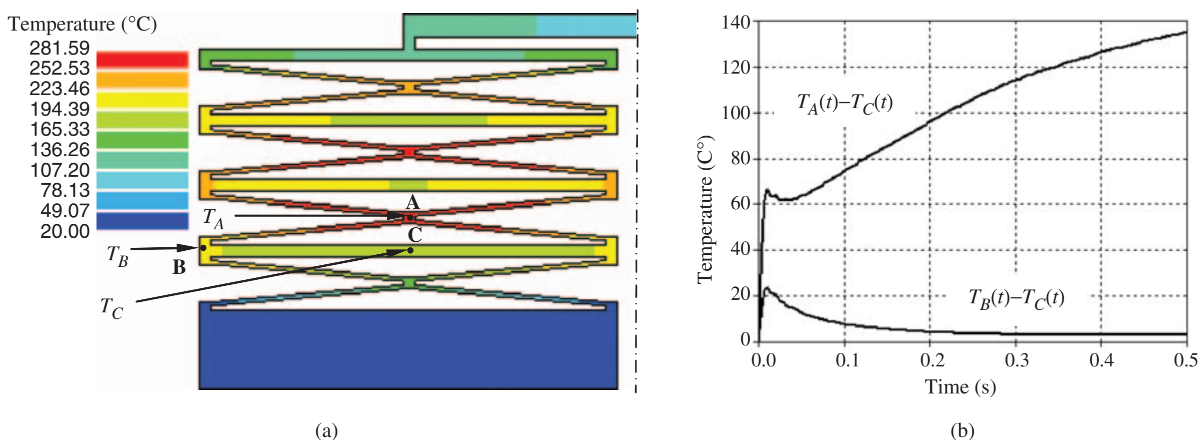

Figure 3. *Simulated electro-thermal performance of the microactuator under an applied voltage of 0.6 V: (a) typical temperature distribution and (b) temperature difference.*

Downloaded from jim.sagepub.com at NATIONAL CHIAO TUNG UNIV LIB on April 26, 2014

small to be used as an actuation motion in functional microdevices. For example, a beam of the dimensions $200(L) \times 10(W) \times 25(T)\,\mu m$, made from commercial pure nickel with a coefficient of linear thermal expansion of $\alpha = 8.5–14.0 \times 10^{-6}\,K^{-1}$ (Cverna, 2002) heated up from 20 to 100°C, expands approximately 0.14–0.22 μm. Therefore, the electro-thermally driven microactuators normally require design elements and structures to further amplify these small motions.

KINEMATICS OF AN ACTUATION UNIT

Figure 4 shows two generalized kinematic models of an actuation unit, where an actuation beam with one degree of freedom (linear extension) can be kinematically modeled as two undeformed links with one prismatic joint. The outer end of each link has a rotary joint providing one degree connection (rotation around the joint) with the constrainer and mirrored actuation beam. The constrainer has a constant length and provides a geometrical constraint acting as a frame preventing transverse motions. Each half of the actuation unit can be modeled as a planar five bar mechanism (Figure 4(a)), or each quarter of the actuation unit can be modeled as a four bar mechanism (Figure 4(b)). The input motions, i.e., small thermal expansions of actuation beams, are converted into larger output in-plane linear motions by the design and kinematics of the actuation unit. The magnification depends on the actuation angle β, between the actuation beam and the constrainer. For smaller angles, the magnification can be approximated by (Hickey et al., 2002; Lai et al., 2004):

$$\frac{1}{\tan\beta} \tag{1}$$

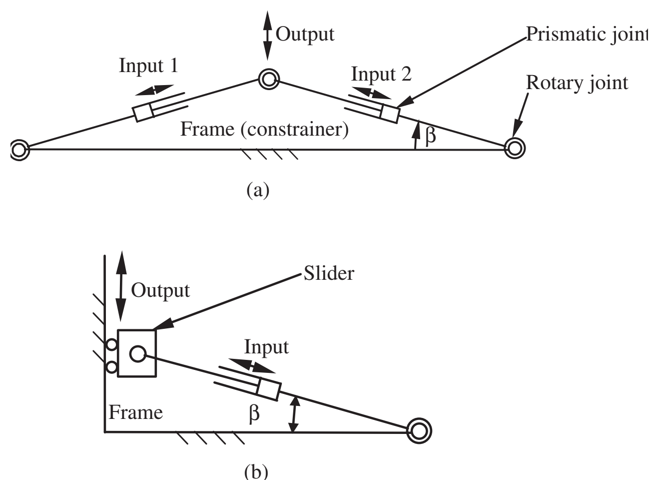

Figure 4. *Kinematics of an actuation unit: (a) five-bar mechanism and (b) four-bar mechanism.*

Thus, decreasing the angle β increases the achievable magnification. For example, for $\beta = 6°$, the approximate magnification is 10 times; for $\beta = 3°$, the magnification is 20 times. These results agree with the simulation results reported in Hsu et al. (2002).

The total output displacement is the accumulation of the resultant output motion of every single actuation unit, whereas each actuation unit experiences the same amount of external load due to the cascaded structure of the actuator. Further, the actuator, formed by two parallel identical cascaded actuation units, would double the output force. To obtain an even larger output force, increasing the number of the actuation beams in each actuation unit placing them in parallel could be a preferred choice.

PERFORMANCE CHARACTERIZATION SETUP AND PROCEDURES

Figure 5 shows an experimental setup for the performance characterization of the fabricated prototype microactuators. The setup consisted of an Agilent™ programmable power supply, digital oscilloscope (LeCroy WaveRunner, LT354), desktop computer, and optical microscope (Olympus, SZX12) with a Basel CMOS camera. All these instruments were connected to the desktop PC and controlled and synchronized in time using in-house developed software – an experiment control program. This program was designed to communicate to the instruments, setup their parameters, record on-line measured data and most important, synchronized their start time, data acquisition, and functioning in time. The microactuator was mounted on a small piece of epoxy circuit board glued to a plastic container and was wired to a standard socket as shown in Figure 6. The actuator was connected to the power supply through a 1 Ω power resistor. Two channels of

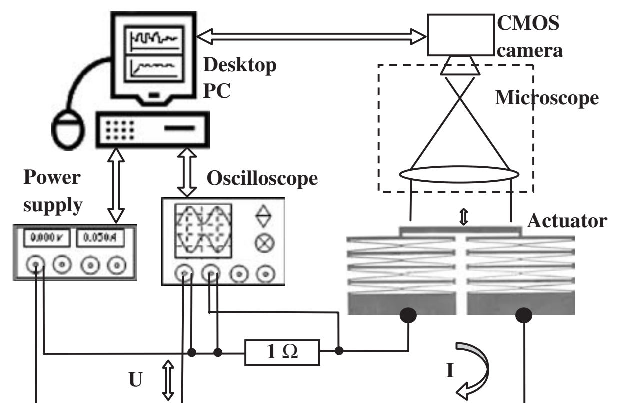

Figure 5. *Experimental setup for performance evaluation.*

Downloaded from jim.sagepub.com at NATIONAL CHIAO TUNG UNIV LIB on April 26, 2014

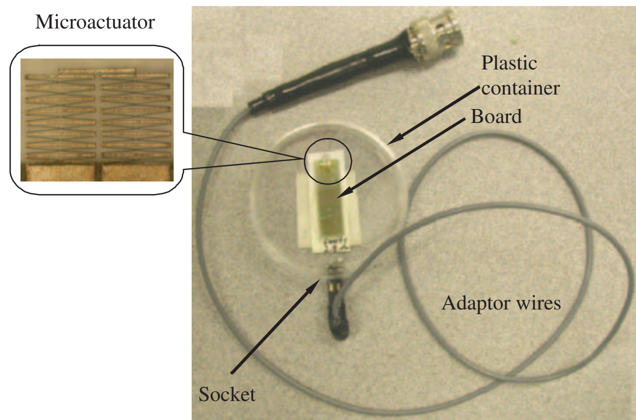

Figure 6. *A mounted microactuator with connection wires.*

the oscilloscope were connected in parallel to the power supply and to the power resistor to measure and record on-line changes in applied voltage and current.

The electro-mechanical performance characterization was performed as a 'step input' testing procedure based on synchronized in time functioning of the power supply and measurements of applied current, generated voltage, and images of the moving actuator by using the experiment control software. The procedure involved the following steps. Once the experiment control program was launched, it configured the CMOS camera and started capturing images of the actuator under test with a speed of 100 frames per second. After the first 100 video frames (1 s) were captured, the computer sends a command to the power supply through USB-GPIB port to switch on to apply a desired current. The oscilloscope was triggered to capture applied current and generated voltage due to rise in current value while the camera continued capturing images. Actuation lasted 3 s (300 video frames) that was sufficient for the actuator to reach its steady state. After that, the computer commanded the power supply to switch off and disconnect the applied current while the camera continued acquiring images for 100 images more (1 s) to record the returning behavior of the actuator. The time duration required for the oscilloscope for gathering data was similar to that of the computer used to capture the images. The captured images were analyzed by National Instrument™ Automation Inspection software to extract the dynamic response and steady state characteristics of the actuator with respect to the applied current. Figure 7 shows typical electric (applied current/voltage versus time) and dynamic (output displacement versus time) responses of the actuator with 6 units with an applied current of 100 mA. These characteristics were measured and used for performance characterization of microactuators with 2, 4, and 6 actuation units.

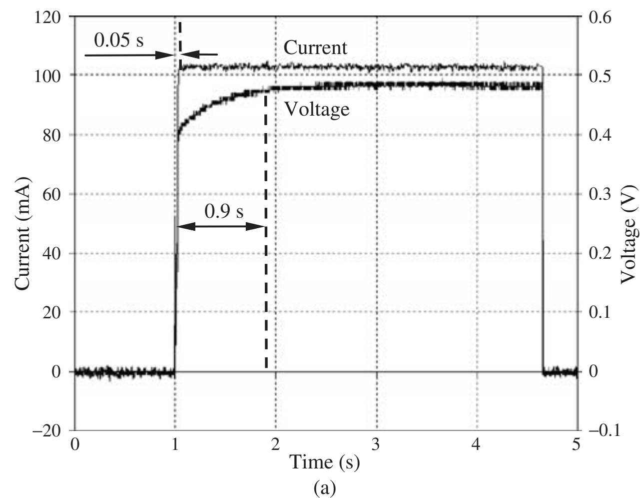

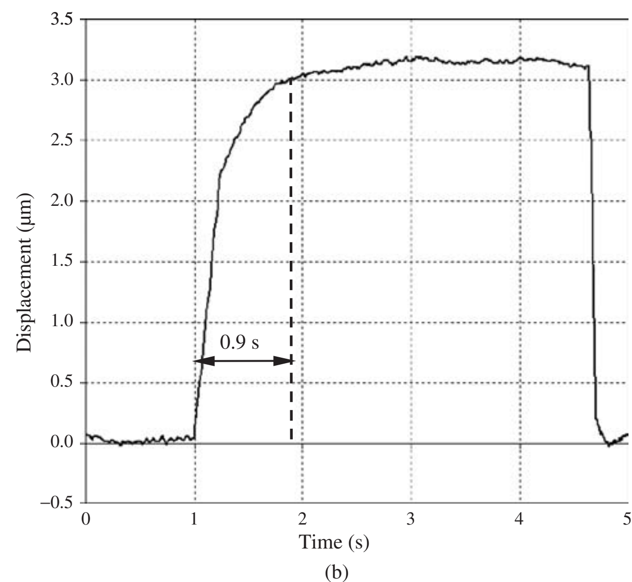

Figure 7. *Typical electric and dynamic responses (microactuator with six actuation units under 100 mA applied current). (a) Electric response (current and voltage vs time) and (b) dynamic response (displacement vs time).*

RESULTS AND ANALYSIS

Static Performance

The static performance of microactuation mechanisms, such as microactuators and microgrippers, is related to the functional relationship between applied electric parameters, e.g., current, voltage, power, and maximum generated displacements. These characteristics are important for the desired design specifications and actual application purposes. Figure 8 shows the static electro-mechanical performance characteristic as a function of maximum output displacements versus applied current and the number of actuation units. The output displacements exponentially increase along with a corresponding increase in the applied current and the number of actuation units. Under the maximum applied driving current of 185 mA, the microactuators

Downloaded from jim.sagepub.com at NATIONAL CHIAO TUNG UNIV LIB on April 26, 2014

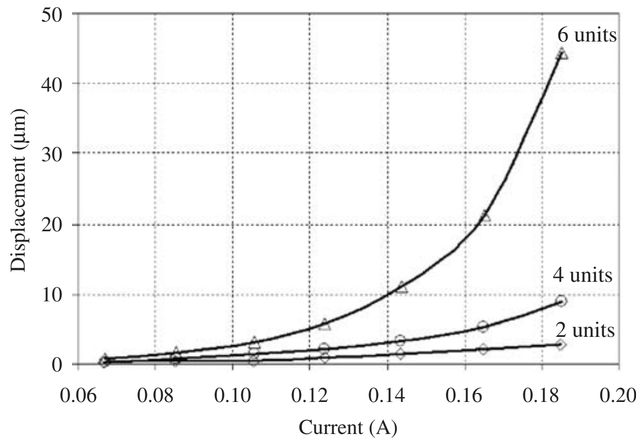

Figure 8. Output displacements with respect to the applied current.

with 2, 4, and 6 actuation units generated output displacement of 2.8, 9.4, and 44.4 μm, respectively. Figure 8 also shows that for the same driving current, the actuator with 6 actuation units has the highest output displacement per actuation unit. For example, at 185 mA, displacements per actuation unit are of the order of 1.4, 2.4, and 7.4 μm for the actuators with 2, 4, and 6 actuation units, respectively.

Figure 9 shows a linear relationship between the output displacement and the input power for input power below 0.2 W. The more actuation units an actuator has, the higher slope the correlation exhibits. The slope of this correlation represents both the effectiveness and efficiency of an actuator in terms of generating output displacements with respect to the consumed power.

The relative displacements in the time domain of each actuation unit for an applied current of 185 mA are shown in Figure 10. It can be seen that the total deflection of 9.39 μm is due to the accumulation of the relative displacements (displacements of two adjacent actuation units) of every single actuation unit. Each actuation unit may generate different relative displacements and contributes to the total output displacement of the actuator because of complex temperature distribution and due to different voltage/power distribution across the entire microactuator design. It was also noticed experimentally for all tested microactuators that the last actuation unit generates significantly larger, 50% more relative displacement than the others as shown in Figure 10. This effect can take place only in the case of the last actuation unit since this unit receives higher applied voltage and higher temperature.

It is also important to note that thermal microactuators fabricated by silicon micromachining process typically exhibit electrical resistances of the order of several kilo ohms (Hickey et al., 2002; Lai et al., 2004) with a resistance of connection wires <1 Ω. Therefore, it can be assumed safely that all the applied voltage was used up in testing the microactuator. Further, the

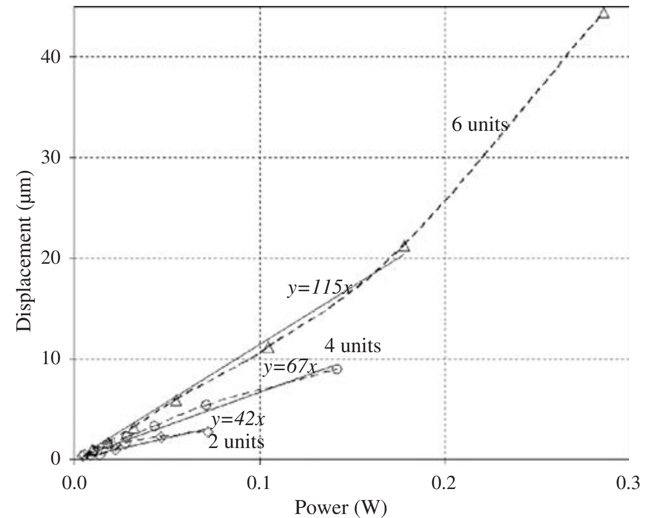

Figure 9. Input power vs output displacement.

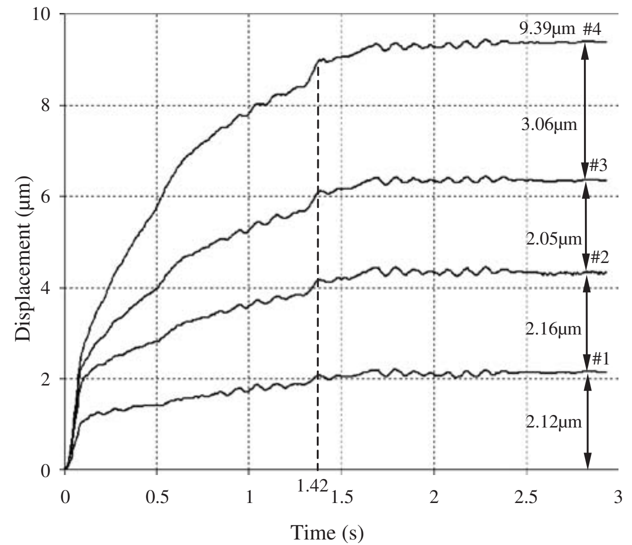

Figure 10. Dynamic characteristics of the actuator with four actuation units and each actuation unit under 185 mA applied current.

resistance increment of silicon microactuators due to Joule heat is insignificant compared to its original resistance. For metal-based microactuators with a monolithic structure presented herein, the actuators have resistance values of only a few ohms, almost the same order as that of the connection wires. When current passes through the actuation beams, the beams will heat up by Joule heating thereby causing an increase in their resistance values. This increment in resistance for metal-based actuators is significant for power consumption and therefore performance. The actual resistance of microactuators during functioning was calculated using measured applied current and voltage, and Figure 11 shows a significant increase in resistance of the actuators with respect to applied current. For instance, the actuators with 2, 4, and 6 actuation units

Downloaded from jim.sagepub.com at NATIONAL CHIAO TUNG UNIV LIB on April 26, 2014

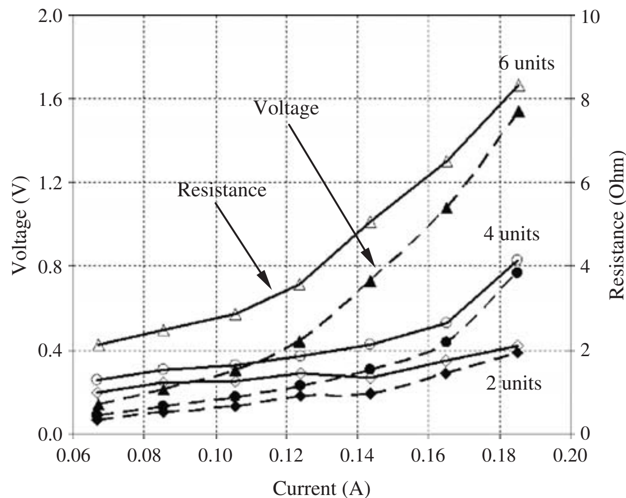

Figure 11. Static electric characteristics of microactuators with 2, 4, and 6 actuation units.

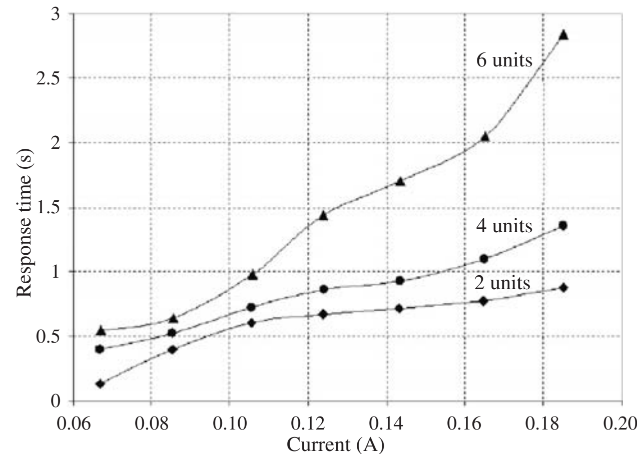

Figure 12. Response times of the actuators under different applied currents.

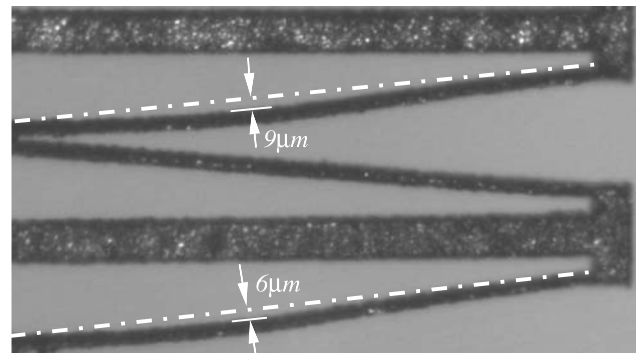

Figure 13. Example of buckled actuation beams.

increased their resistance values from 0.99, 1.29, and 2.13 Ω to 2.1, 4.15, and 8.34 Ω, respectively, when the current increased from 60 to 180 mA. The resistance increments of the actuators with 2, 4, and 6 actuation units increases as the number of actuation units non-linearly increases, which could be the result of the complex temperature distribution along the structure.

Dynamic Performance

According to the control theory, the dynamic performance of a system always characterizes a transient system behavior between two steady states. In the case of electro-thermally driven microactuators, the dynamic performance is an electro-thermo-mechanical response as a step response function on a constant applied current as a step input function. A knowledge of the step response function is an essential element for mathematical modeling and close-loop control of the system. In this study, the step response functions as a dynamic characteristics of the actuator was analyzed.

In general, the dynamic performance of the electrically driven microactuator can be fully characterized by three interrelated dynamic responses on applied current: (a) electric response with respect to a consumed voltage, (b) dynamic response with respect to an output displacement, and (c) thermal response with respect to generated heat/temperature. Figure 7 confirms interrelation of the measured electric and dynamic responses by identical response time of 0.9 s.

Figure 10 shows an example of dynamic responses of a microactuator with four actuation units for an applied current of 185 mA. It was observed that all the response curves have similar periodic characters without oscillations and overshoots that were expected as for typical electro-thermal systems. Each unit of the actuator took the same time of approximately 1.4 s to reach the steady state (Figure 10) that characterizes the static performance of the microactuator.

The response time of the actuators with 2, 4, and 6 actuation units for different applied currents was studied (Figure 12). The experiments showed that the response time significantly depended on the number of actuation units and the applied current. It was demonstrated that for the same magnitude of applied current, the actuator with more actuation units requires a longer time to reach the steady state position. For example, the actuators with 2, 4, and 6 under 120 mA applied current had response times of 0.7, 0.9, and 1.4 s, respectively. Further, for a typical actuator, the response time significantly increases with an increase in applied current, e.g., response time of 4.7 times longer, from 0.6 to 2.8 s, after 3 times increase in applied current, from 0.06 to 0.18 A, was observed for the actuator with six actuation units.

Buckling Effect

During the experiments, buckling effects occurred when driving current was increased beyond 0.25 A. Figure 13 shows buckled actuation beams with buckling offsets of 6 and 9 μm from the original positions.

Downloaded from jim.sagepub.com at NATIONAL CHIAO TUNG UNIV LIB on April 26, 2014

Table 2. Comparison of selected nickel-based microactuators.

Parameters	Selected Ni-based microactuators for comparison		
	Reference (Que et al., 2001a)	Reference (Hsu et al., 2002)	Present study
Number of sub-actuation units	1	10	8
Dimensions of the actuation beams			
Width (μm)	6	8	10
Height (μm)	3	11	25
Length (μm)	410	1000	1000
Actuation angle (degree)	2.89°	1°	5°
Max displacement (μm)	10	200	9
Max displacement per actuation unit (μm)	10	20	1.125
Max input power per actuation unit (mW)	140	66*	18
Resistance of the entire actuator (Ω)	5.5	13.7*	4 (max)
Method of fabrication	Electroplate	Electroplate	Laser

*These are calculated approximations.

The buckling effect could be explained as follows. All actuation beams are slender under longitudinal axial compression loads. These may include internal deformation loads, external loads, or their combination. With the continuous increase in the applied current, the actuation beam continuously generates larger thermal expansion and therefore, the output motion is directed against the increasing internal (from thermal expansion) and/or external (from interconnected actuation units) axial loads. Once the axial load exceeds a critical value, the beam becomes elastically unstable (Juvinall and Marshek, 1991) and buckling sets in, causing permanent deformations within the original geometry of the actuation beam, as shown in Figure 13. These deformations reduce the output force and displacement values, and may cause the eventual failure of the actuator.

Comparison with other Observations

For benchmarking purposes, the microactuator with four actuation units was compared with the Ni-based actuators presented in (Que et al., 2001a) and (Hsu et al., 2002) in terms of maximum output displacements and power consumption with respect to the geometric dimensions. Also, the sub-basic unit of the microactuators was defined as a chevron shape formed by two single actuation beams. Thus, a basic actuation unit of the microactuators in (Hsu et al., 2002) and in the present article has two sub-basic actuation units. Table 2 lists compared characteristics.

It was shown in the Section 'Kinematics of an Actuation Unit' that the output displacement increases as the actuation angle β decreases. As expected, the microactuator in (Hsu et al., 2002) generates the largest output motion because of its sharply oriented beam angle of 1°. The critical load of a slender beam P_{cr} is given by (Juvinall and Marshek, 1991)

$$P_{cr} = \frac{\pi^2 EI}{L_e^2} \tag{2}$$

where E is the modulus of elasticity, I is the moment of inertia of the cross-section with respect to the buckling–bending axis; L_e denotes the equivalent length of a column. The microactuators studied in this article have a higher value of I due to a larger cross-sectional area. Therefore, they can carry a larger compression load and provide better in-plane performance such as anti-buckling and are also free from out-of-plane bending. Also, the larger cross-sectional area enables a significantly larger force, e.g., our experimental results show that the microactuator with four actuation units produced ≈2 mN force with a driving current of 185 mA.

CONCLUSIONS

In the present article, a systematic study of the electromechanical performance of the in-plane electrothermally driven linear microactuators is presented. A set of microactuators with different number of actuation units, in particular, 2, 4, and 6 were fabricated from a nickel foil with a thickness of 25 μm, and accuracy and precision within ±1 μm using the high-precision laser microfabrication technology. The static and dynamic performance of the prototype microactuators were analyzed with respect to the maximum output displacements, electric power consumption, and functional efficiency. The maximum in-plane displacement values of 2.8, 9.4, and 44.4 μm were achieved for the current value of 185 mA for these three actuators.

The following conclusions can be drawn from these studies:

1. The analyzed microactuator is a highly efficient miniature mechanism with complex static and dynamic performance and capable of generating output displacements reliably and of the order of atleast 4% of its linear dimension with a maximum power consumption of 0.2 W.

Downloaded from jim.sagepub.com at NATIONAL CHIAO TUNG UNIV LIB on April 26, 2014

2. The high actuation performance of the each actuation unit is a result of an innovative combination of the rhombus-shaped design and the electric equivalent of Wheatstone bridge formed by the resistance values of the four actuation beams.
3. The efficiency of the microactuators depends on the number of actuation units in each cascaded structure. In general, an actuator with more actuation units produces larger output displacements, but this functional relationship is non-linearly proportional to the number of actuation units.
4. The efficiency of the single actuation unit depends on the number of such actuation units coupled in the cascaded structure. The output displacement and the electric power consumption per actuation unit increase with the number of actuation units.
5. The reliable static performance of each microactuator has exponential character with respect to the applied current and it is limited by the buckling of the actuation beams when the compression load exceeds the thermal expansion force.
6. The dynamic response time of actuators depends and increases with an increase in the number of the actuation units and in the applied current.
7. The experimental results validate the basis for modeling and design optimization of the toggled electro-thermal microdevices.

These results strengthen the usefulness of the prototype microactuators for applications in MEMS/MOEMS, microfluidic, and microrobotic devices.

ACKNOWLEDGMENTS

The authors are grateful to Mahmud-Ul Islam, Director, Production Technology Research, IMTI, for his continued support in this work. Also, thanks are due to Marco Zeman, Matthew Hsu, and Hugo Reshef, for their help in performing the laser micromachining work and in optimizing the process parameters, and to Raj Vatsya for critical comments and corrections. This work was funded by NRC (Canada) – NSC (Taiwan) Collaborative Research Program and partially by NSERC Discovery Grant R3440A01.

REFERENCES

Bordatchev, E., Nikumb, S. and Hsu, W. 2002. "Fabrication of Long-stretch Microdrive for MEMS Applications by Ultra Precision Laser Micromachining," In: *Proceedings of the Canada–Taiwan Workshop on Advanced Manufacturing Technologies*, September 23–24, London, Ontario, Canada, pp. 243–251.

Bordatchev, E.V. and Nikumb, S.K. 2005. "Electro-thermally Driven Microgrippers for MEMS Applications," *Journal of Microlithography, Microfabrication, and Microsystems*, 4(2): 023011, 7 pp.

Bordatchev, E., Nikumb, S. and Hsu, W. 2004. "Laser Micromachining of the Miniature Functional Mechanisms, in Photonics North 2004: Photonic Applications in Astronomy, Biomedicine, Imaging, Materials Processing, and Education," In: *Proceedings of SPIE*, SPIE, Bellingham, WA, Vol. 5578, pp. 579–588.

Braun, A. and Zimmer, K. 2001. "Fabrication of MEMS Structures by Laser Micromachining," In: *Proceedings of SPIE*, Vol. 4236, pp. 213–221.

Comtois, J., Bright, V. and Phipps, M. 1995. "Thermal Microactuators for Surface-micromachining Processes," *Processing of the SPIE*, 2642:10–21.

Cragun, R. and Howell, L.L. 1999. "Linear Thermal–Mechanical Microactuators," *ASME, IMECE MEMS*, pp. 181–188.

Cverna, F. 2002. *Thermal Properties of Metals*, ASM International, Materials Park, Ohio, ISBN: 0-87170-768-3.

Debeda, H., Freyhold, T., Mohr, J., Wallrabe, U. and Wengelink, J. 1999. "Development of Miniaturized Piezoelectric Actuators for Optical Applications Realized Using LIGA Technology," *J. MEMS*, 8(3):258–263.

Gianchandani, Y.B. and Najafi, K. 1996. "Bent-beam Strain Sensors," *J. Micromech. Microeng*., 5(1):52–58.

Grade, J., Jerman, H. and Kenny, T. 2003. "Design of Large Deflection Electrostatic Actuators," *J. MEMS*, 12(3):335–343.

Guckel, H., Klein, J., Christerson, T., Skrobis, K., Laudon, M. and Lovell, E.G. 1992. "Thermo-magnetic Metal Flexure Actuators," In: *Technical Digest, Solid State Sensors and Actuators Workshop*, Hilton Head, SC, pp. 73–75.

Harness, T. and Syms, R.R.A. 2000. "Characteristic Modes of Electrostatic Comb-drive X-Y Microactuators," *Journal of Micromechanics and Microengineering*, 10:7–14.

Hickey, R., Kujath, M. and Hubbard, T. 2002. "Heat Transfer Analysis and Optimization of Two-beam Microelectromechanical Thermal Actuators," *J. Vac. Sci. Technol. A*, 20:971–974.

Hsu, T.-R. 2002. *MEMS & Microsystems: Design and Manufacturing*, McGraw-Hill, New York.

Hsu, C., Tai, W. and Hsu, W. 2002. "Design and Analysis of an Electro-thermally Driven Long-stretch Micro Drive with Cascaded Structure," In: *Proceedings of IMECE2002 ASME International Mechanical Engineering Congress and Exposition*, November 17–22, 2002, New Orleans, Louisiana, USA, pp. 235–240.

Huang, Q. and Lee, K. 1999. "Analysis and Design of Polysilicon Thermal Flexure Actuator," *J. Micromech. Microeng*., 9:64–70.

Juvinall, R. and Marshek, K. 1991. *Fundamentals of Machine Components Design*, 2nd edn, John Wiley & Sons, Inc., pp. 186–190.

Klaassen, E.H., Peterson, K., Noworolski, M., Logan, J., Maluf, N., Brown, J., Storment, C., McCulley, W. and Kovacs, G. 1995. "Silicon Fusion Bonding and Deep Reactive Ion Etching: A New Technology for Microstructures Transducers'95," In: *8th Int. Conf. on Solid-State Sensors and Actuators, and Eurosensors IX*, Stockholm, Sweden, pp. 25–29.

Koester, D.A., Mahadevan, R., Hardy, B. and Markus, K. *MUMPs Design Handbook*, Revision 7.0 (Triangle Park, NC: Cronos Integrated Microsystems).

Lai, Y., McDonald, J., Kujath, M. and Hubbard, T. 2004. "Force, Deflection and Power Measurements of Toggled Micro Thermal Actuators," *J. Micromech. Microeng*., 14:49–56.

Luo, J.K., Flewitt, A.J., Spearing, S.M., Fleck, N.A. and Milne, W.I. 2004. "Modelling of Microspring Thermal Actuator," In: *Proceedings of the NSTI Nanotechnology Conference and Trade Show*, pp. 355–358.

Luo, J.K., Flewitt, A.J., Spearing, S.M., Fleck, N.A. and Milne, W.I. 2005. "Three Types of Planar Structure Microspring Electro-thermal Actuators with Insulating Beam Comstrains," *J. Micromech. Microeng*., 15:1527–1535.

Que, L., Park, J. and Gianchandani, Y.B. 2001a. "Bent–beam Electrothermal Actuators: Part I. Single Beam and Cascaded Devices," *J. MEMS*, 10:247–254.

Downloaded from jim.sagepub.com at NATIONAL CHIAO TUNG UNIV LIB on April 26, 2014

Que, L., Park, J.-S. and Gianchandani, Y.B. 2001b. ''Bent-Beam Electrothermal Actuators – Part I: Single Beam and Cascaded Devices,'' *J. Micromech. Microeng*., 10(2):247–253.

Sinclair, M.J. 2000. ''A High Force Low Area MEMS Thermal Actuator,'' In: *Inter. Society Conf. on Thermal phenomena*, pp. 127–132.

Syms, R.R.A., Zou, H. and Stagg, J. 2004. ''Robust Latching MEMS Translation Stages for Microoptical Systems,'' *J. Micromech. Microeng*., 14:667–674.

Williams, K., Maluf, N., Fuller, N., Barron, R., Jaeggi, D. and van Drieenhuizen, B. 1999. ''A Silicon Microvalve for the Proportional Control of Fluids,'' In: *10th Int. Conf. on Solid-state Sensors and Actuators* (Transducers' 99), Sendai, Japan, pp. 1804–1807.

Ye, W., Mukherjee, S. and MacDonald, N. 1998. ''Optimal Shape Design of an Electrostatic Comb Drive in Microelectromechanical Systems,'' *J. MEMS*, 7(1):16–26.

Downloaded from jim.sagepub.com at NATIONAL CHIAO TUNG UNIV LIB on April 26, 2014